

Resonant Spin Excitation in an Overdoped High Temperature Superconductor

H. He¹, Y. Sidis², P. Bourges², G.D. Gu³, A. Ivanov⁴, N. Koshizuka⁵, B. Liang¹,
C.T. Lin¹, L. P. Regnault⁶, E. Schoenher¹, and B. Keimer^{1,7}

¹ *Max-Planck-Institut für Festkörperforschung, 70569 Stuttgart, Germany.*

² *Laboratoire Léon Brillouin, CEA-CNRS, CE-Saclay, 91191 Gif sur Yvette, France.*

³ *Department of Advanced Electronic Materials, School of Physics,
University of New South Wales, Sydney 2052, Australia.*

⁴ *Institut Laue Langevin, 156X, 38042 Grenoble cedex 9, France.*

⁵ *SRL/ISTEC, 10-13, Shinonome 1-chome, Koto-ku, Tokyo 135, Japan.*

⁶ *CEA Grenoble, Département de Recherche Fondamentale sur la
Matière Condensée, 38054 Grenoble cedex 9, France.*

⁷ *Department of Physics, Princeton University, Princeton, NJ 08544, USA.*

(December 2, 2024)

An inelastic neutron scattering study of overdoped $\text{Bi}_2\text{Sr}_2\text{CaCu}_2\text{O}_{8+\delta}$ ($T_c = 83$ K) has revealed a resonant spin excitation in the superconducting state. The mode energy is $E_{\text{res}} = 38$ meV, significantly lower than in optimally doped $\text{Bi}_2\text{Sr}_2\text{CaCu}_2\text{O}_{8+\delta}$ ($T_c = 91$ K, $E_{\text{res}} = 43$ meV). This observation, which indicates a constant ratio $E_{\text{res}}/k_B T_c \sim 5.4$, helps resolve a long-standing controversy about the origin of the resonant spin excitation in high-temperature superconductors.

A resonant spin excitation [1–8] with wave vector (π, π) has recently emerged as a key factor in the phenomenology of the copper oxide superconductors. In particular, prominent features in angle-resolved photoemission [9–11] and optical conductivity [12,13] spectra have been attributed to interactions of this bosonic mode with fermionic quasiparticles. The implications of these observations for the mechanism of high temperature superconductivity are under intense scrutiny, especially following suggestions that spectral weight of the mode (which is present only below the superconducting transition temperature, T_c [3,4]) provides a measure of the condensation energy [14,15] or condensate fraction [16] of the superconducting state. Several fundamentally different microscopic descriptions of the neutron data have been proposed. Some of these [3,17] attribute the resonance peak to the threshold of the particle-hole (ph) spin-flip continuum at $\lesssim 2\Delta_{\text{SC}}$ where Δ_{SC} is the energy gap in the superconducting state, others [11,18,19] to a magnon-like collective mode whose energy is bounded by the gap. Although the starting points of these calculations are disparate (itinerant band electrons in [11,17,18], localized electrons in [19]), the excitations corresponding to the neutron peak are described by the same quantum numbers (spin 1 and charge 0). In a completely different approach [20], the neutron data are interpreted in terms of a collective mode in the particle-particle (pp) channel whose quantum numbers are spin 1 and charge 2. The pp continuum that provides the upper bound for the pp resonance in the latter model is unaffected by superconductivity. Despite the central significance of this issue, there is still no “smoking gun” experiment selecting the correct theoretical approach.

A careful measurement of the doping dependence of the mode energy, E_{res} , can resolve this issue decisively.

In Refs. [18–20], the mode is interpreted as a soft mode whose energy is expected to decrease as a magnetic instability is approached with decreasing hole content. This is made explicit in an expression derived from the pp model which predicts that E_{res} is proportional to the doping level [20]. The behavior observed in underdoped $\text{YBa}_2\text{Cu}_3\text{O}_{6+x}$ [5–7] is consistent with that prediction. This alone, however, does not amount to a “smoking gun” because it can also be understood in the framework of the simple ph pair production model where $E_{\text{res}} \propto \Delta_{\text{SC}} \propto T_c$. In underdoped samples, T_c in turn is monotonically related to the hole content. Further difficulties derive from ambiguities associated with the distinction between the normal-state “pseudo-gap” in the charge sector and the true superconducting gap in the underdoped state. These are mirrored in the spin sector by uncertainties regarding the relationship between a broad peak observed by neutron scattering in the normal state [5–7] and the sharp resonant peak in the superconducting state.

The neutron data on underdoped samples therefore do not discriminate clearly between the very different theories of the resonance peak. Here we report a neutron scattering study in the overdoped state of $\text{Bi}_2\text{Sr}_2\text{CaCu}_2\text{O}_{8+\delta}$ where none of these complicating factors are present. In particular, T_c is reduced while the hole content keeps increasing, and the normal-state pseudogap disappears.

To this end, we used an array comprising eight small (individual volumes ~ 0.03 cm³), high quality overdoped $\text{Bi}_2\text{Sr}_2\text{CaCu}_2\text{O}_{8+\delta}$ single crystals grown by the floating-zone method [21]. In their as-grown state, the crystals were optimally doped, with $T_c \sim 91$ K, as was the sample used for our previous neutron study [8]. Using established procedures [22], they were subsequently annealed at 650°C under oxygen flow for 200 hours. (The long annealing time was used as a precaution. Previous studies

[22] have shown that 20 hours are sufficient to achieve a homogeneous oxygen content for identically prepared samples.) Following this, the individual samples exhibited sharp (width 5-7 K) superconducting transitions at 83 K, in excellent agreement with prior results [22]. The crystals were co-aligned by x-ray Laue diffraction and mounted in an aluminum holder. The overall mosaicity of the array, $\sim 5^\circ$, was comparable to the angular dependence of the magnetic signal of the previous study [8] and therefore of little consequence for the signal intensity. However, compared to our previous experiment on a monolithic, optimally doped single crystal, the imperfect alignment of the crystal array would introduce additional uncertainties into an absolute intensity unit calibration which will therefore not be given here. In order to establish an optimal basis for a comparison of the results on optimally doped and overdoped samples, the experimental setup precisely duplicated the one used for the previous study [8]. The experiments were conducted on the triple axis spectrometer IN8 (at the Institut Laue-Langevin in Grenoble, France) in a focusing configuration with Cu(111) monochromator, pyrolytic graphite (002) analyzer, and 35 meV fixed final energy. The wave vector $Q = (H, K, L)$ is given in reciprocal lattice units (r.l.u.), that is, in units of the reciprocal lattice vectors $a^* \sim b^* \sim 1.64 \text{ \AA}^{-1}$ and $c^* \sim 0.20 \text{ \AA}^{-1}$. In these units, the in-plane wave vector (π, π) is equivalent to $(\frac{h}{2}, \frac{k}{2})$ with h, k odd integers. The data were taken with L set close to the maximum of the intensity modulation due to magnetic coupling of the bilayers ($L = -13.2$ or $L = -14$ for $\text{Bi}_2\text{Sr}_2\text{CaCu}_2\text{O}_{8+\delta}$ [8]).

$\text{Bi}_2\text{Sr}_2\text{CaCu}_2\text{O}_{8+\delta}$ is a highly complex material with a multitude of densely spaced phonon branches, not to mention the additional lattice dynamical complexity due to the incommensurate modulation of the Bi-O layer. Raw neutron data therefore show a large, featureless background predominantly due to unresolved single-phonon events. An example is given in Fig. 1. Building on lessons drawn from work on $\text{YBa}_2\text{Cu}_3\text{O}_{6+x}$, we have previously established [8] how the magnetic signal can be separated from this background by virtue of its characteristic energy, momentum, and temperature dependences. Specifically, the magnetic resonance peak that is the primary focus of the present study gives rise to a magnetic signal at wave vector $Q = (\pi, \pi)$ that is present only below T_c (Refs. [3–6,8]). The first step therefore involves taking the difference between the measured spectra in the superconducting and normal states and studying the energy and wave vector dependence of the enhanced signal. Figs. 2 and 3 show that this is confined to a narrow region in energy and wave vector centered at $E = 38 \text{ meV}$ and $Q = (\pi, \pi)$, while the background away from this region is reduced upon cooling. (The temperature dependence of the background becomes more pronounced at low energies, because the phonon scattering follows the Bose population factor $(1 - \exp(-E/k_B T))^{-1}$.)

This is precisely the signature of the magnetic resonance peak observed in $\text{YBa}_2\text{Cu}_3\text{O}_{6+x}$ and optimally doped $\text{Bi}_2\text{Sr}_2\text{CaCu}_2\text{O}_{8+\delta}$. In fact, the only difference between the present data and those on the latter material, where the peak occurs at 43 meV (dashed line in Fig. 2), is the noticeable energy shift which is the central result of this paper. The widths in wave vector ($\Delta Q \sim 0.5 \text{ \AA}^{-1}$ full width at half maximum) and energy ($\Delta E \sim 10 \text{ meV}$) of the resonance peaks in optimally doped [8] and overdoped $\text{Bi}_2\text{Sr}_2\text{CaCu}_2\text{O}_{8+\delta}$ are identical to within the experimental error. Hence, there is no indication that extrinsic factors (such as an increased number of defects created by post-annealing) could be responsible for the observed energy shift.

Before discussing the implications of these data, we proceed to the second step in the identification of the resonance peak, namely, the determination of the onset temperature of the magnetic signal. The temperature dependence of the peak magnetic intensity, shown in Fig. 4, indeed exhibits the strong upturn around $T_c = 83 \text{ K}$ that characterizes the resonance peak. Interestingly, this upturn is even sharper here than in the optimally doped sample. As in optimally doped $\text{YBa}_2\text{Cu}_3\text{O}_7$ (Refs. [3,4]) and $\text{Bi}_2\text{Sr}_2\text{CaCu}_2\text{O}_{8+\delta}$ (Ref. [8]), there is no evidence of magnetic scattering above T_c although this determination is limited by the high nuclear background.

The data shown in Figs. 2-4 are an essential complement to an extensive data set on the resonance peak in underdoped $\text{YBa}_2\text{Cu}_3\text{O}_{6+x}$. A representative subset [5–7] is shown in Fig. 5 along with the presently available data on $\text{Bi}_2\text{Sr}_2\text{CaCu}_2\text{O}_{8+\delta}$. While we did not confirm the linear relationship between E_{res} and doping level predicted by the pp model of the resonance peak [20], Fig. 5 suggests that the parameter controlling E_{res} is actually the transition temperature T_c , with $E_{\text{res}}/k_B T_c \sim 5.4$. This is the behavior expected on the basis of the simplest possible interpretation of the resonance peak [3,17] that attributes it to a ph excitation across the d -wave superconducting gap (which in turn should be proportional to T_c , at least in overdoped samples where the pseudogap disappears). Qualitatively, our observation is also consistent with more elaborate models incorporating interactions between the particle and hole in the final state. If these are strong enough, a magnon-like collective mode is pulled below the continuum [11,18,19]. Although we are not aware of any explicit predictions, a smooth crossover to the pair production scenario is plausible in the overdoped state as the interaction strength is reduced. Of course, detailed calculations and a direct measurement of the superconducting gap in our $\text{Bi}_2\text{Sr}_2\text{CaCu}_2\text{O}_{8+\delta}$ samples are ultimately required as a confirmation. Reconciling our observation with the pp model would be considerably more difficult, because it directly contradicts the prediction [20] that parameters related to the superconducting state (such as Δ_{SC} and T_c) play no role in deter-

mining E_{res} . It remains to be seen, however, if recently proposed modified versions of the original pp model [24] will lead to different predictions for E_{res} .

Our result also supports the conclusion of a neutron scattering study [23] of 3%-Ni substituted $\text{YBa}_2\text{Cu}_3\text{O}_7$ ($T_c=80$ K). Ni substitution is known to reduce T_c but does not affect the hole content. In $\text{YBa}_2(\text{Cu}_{0.97}\text{Ni}_{0.03})_3\text{O}_7$, E_{res} is shifted from 40 meV to ~ 35 meV so that the ratio E_{res}/T_c is preserved, as observed here for overdoped $\text{Bi}_2\text{Sr}_2\text{CaCu}_2\text{O}_{8+\delta}$.

In conclusion, our experiment clearly favors the ph over the pp interpretation of the resonance peak, at least in its present form, and thus helps resolve a long-standing theoretical controversy. The results reported here will also help confirm and extend promising attempts [9,10,12,13] to develop a unified phenomenology of magnetic and charge spectroscopies of the cuprates.

We gratefully acknowledge discussions with P.W. Anderson, S. Chakravarty, A. Chubukov, E. Demler, W. Hanke, D. Morr, F. Onufrieva, P. Pfeuty, D. Pines, and S. Sachdev. The work at Princeton University was supported by the National Science Foundation under DMR-9809483.

[1] J. Rossat-Mignod *et al.*, Physica C **185-189**, 86 (1991).
[2] H.A. Mook *et al.*, Phys. Rev. Lett. **70**, 3490 (1993).
[3] H.F. Fong *et al.*, Phys. Rev. Lett. **75**, 316 (1995); Phys. Rev. B **54**, 6708 (1996).
[4] P. Bourges *et al.*, Phys. Rev. B **53**, 876 (1996).
[5] P. Bourges, in *The Gap Symmetry and Fluctuations in High Temperature Superconductors*, edited by J. Bok, G. Deutscher, D. Pavuna and S.A. Wolf. (Plenum Press, 1998) 349.
[6] H.F. Fong *et al.*, cond-mat/9910041, and references therein.
[7] P. Dai *et al.*, Science **284**, 1344 (1999).
[8] H.F. Fong *et al.*, Nature **398**, 588 (1999).
[9] Z.X. Shen and J.R. Schrieffer, Phys. Rev. Lett. **78**, 1771 (1997).
[10] J.C. Campuzano *et al.*, Phys. Rev. Lett. **83**, 3709 (1999); M.R. Norman and H. Ding, Phys. Rev. B **57**, R11089 (1998).
[11] A. Abanov and A.V. Chubukov, Phys. Rev. Lett. **83**, 1652 (1999).
[12] D. Munzar, C. Bernhard, and M. Cardona, Physica C **318**, 547 (1999).
[13] J.P. Carbotte, E. Schachinger, and D.N. Basov, Nature **401**, 354 (1999).
[14] D.J. Scalapino and S.R. White, Phys. Rev. B **58**, 8222 (1998).
[15] E. Demler and S.C. Zhang, Nature **396**, 733 (1998).
[16] S. Chakravarty and H.K. Kee, cond-mat/9908205.
[17] See, *e.g.*, L. Yin, S. Chakravarty and P.W. Anderson, Phys. Rev. Lett. **78**, 3559 (1997); A.A. Abrikosov, Phys.

Rev. B **57**, 8656 (1998).
[18] See, *e.g.*, I.I. Mazin and V.M. Yakovenko, Phys. Rev. Lett. **75**, 4134 (1995); F. Onufrieva, Physica C **251**, 348 (1995); D.L. Liu, Y. Zha and K. Levin, Phys. Rev. Lett. **75**, 4130 (1995); N. Bulut and D.J. Scalapino, Phys. Rev. B **53**, 5149 (1996); A.J. Millis and H. Monien, Phys. Rev. B **54**, 16172 (1996); J. Brinckmann and P.A. Lee, Phys. Rev. Lett. **82**, 2915 (1999); F. Onufrieva and P. Pfeuty, cond-mat/9903097.
[19] A.V. Chubukov, S. Sachdev, and J. Ye, Phys. Rev. B **49**, 11919 (1994); D.K. Morr and D. Pines, Phys. Rev. Lett. **81**, 1086 (1998); S. Sachdev, C. Buragohain, and M. Vojta, Science **286**, 2479 (1999).
[20] E. Demler and S.C. Zhang, Phys. Rev. Lett. **75**, 4126 (1995); E. Demler, H. Kohno, and S.C. Zhang, Phys. Rev. B **58**, 5719 (1998).
[21] G.D. Gu, K. Takamuku, N. Koshizuka, and S. Tanaka, J. Crystal Growth **130**, 325 (1998).
[22] S.H. Han *et al.*, Physica C **246**, 22 (1995).
[23] Y. Sidis *et al.*, cond-mat/9912214.
[24] S.C. Zhang *et al.*, Phys. Rev. B **60**, 13070 (1999).

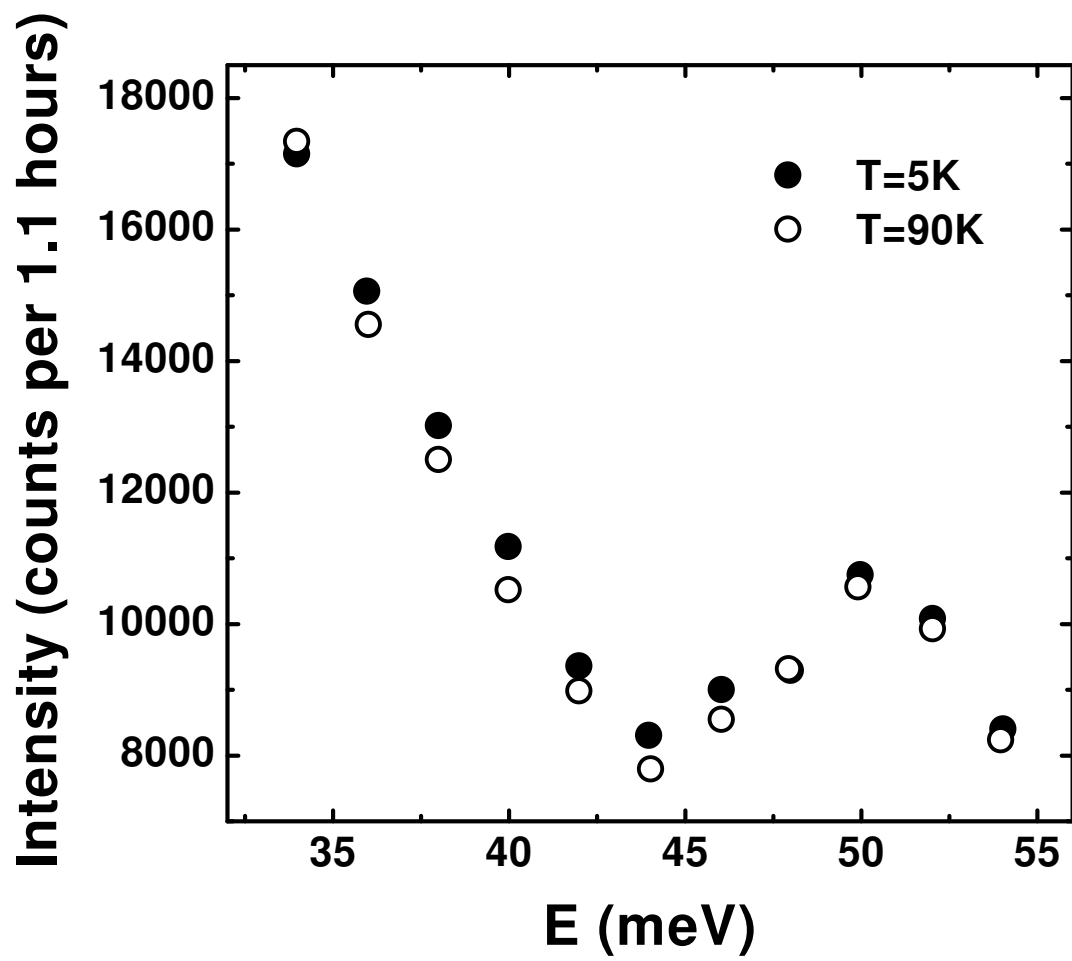
FIG. 1. Raw (unsubtracted) spectra at wave vector $\mathbf{Q} = (0.5, 0.5, -14)$ and temperatures 10K and 100K. The large background is mostly due to a multitude of unresolved phonons (see text).

FIG. 2. Difference spectrum of the neutron intensities at $T = 5$ K ($< T_c$) and $T = 90$ K ($> T_c$), at wave vector $\mathbf{Q} = (0.5, 0.5, -13.2)$. The bar represents the instrumental energy resolution, the line is a guide-to-the-eye. The dashed line represents the resonance energy extracted from a fit to similar data on optimally doped BSCO resonance peak [8].

FIG. 3. Difference spectrum of the neutron intensities at $T = 5$ K ($< T_c$) and $T = 90$ K ($> T_c$), at energy 38 meV. The bar represents the instrumental momentum resolution, the line is a guide-to-the-eye.

FIG. 4. Temperature dependence of the neutron intensity at energy 38 meV and wave vector $\mathbf{Q} = (0.5, 0.5, -13.2)$. The intensity falls to background level above $T_c = 83$ K. The line is a guide-to-the-eye.

FIG. 5. A synopsis of the resonance peak energy E_{res} in $\text{YBa}_2\text{Cu}_3\text{O}_{6+x}$ (open symbols, with squares from Ref. [5], circles from Ref. [6], and diamonds from Ref. [7]) and $\text{Bi}_2\text{Sr}_2\text{CaCu}_2\text{O}_{8+\delta}$ (closed symbols, from Ref. [8] and present work), plotted as a function of the superconducting transition temperature T_c . The errors bars, where given, are measures of (or upper bounds on) the intrinsic width of the peak, *not* of the accuracy to which the peak position is known which is much higher.



I(5K)-I(90K) Q=(0.5,0.5,-13.2)

